Front. Optoelectron. 2015, 8(3): 252–268
DOI 10.1007/s12200-015-0539-2

REVIEW ARTICLE

$Cu_2ZnSn(S,Se)_4$ thin film solar cells fabricated with benign solvents

Cheng ZHANG[1,2], Jie ZHONG (✉)[1,2], Jiang TANG (✉)[2]

1 State Key Laboratory of Advanced Technology for Materials Synthesis and Processing, Wuhan University of Technology, Wuhan 430070, China
2 Wuhan National Laboratory for Optoelectronics, Huazhong Univesity of Science and Technology, Wuhan 430074, China

Abstract $Cu_2ZnSn(S,Se)_4$ (CZTSSe) is considered as the promising absorbing layer materials for solar cells due to its earth-abundant constituents and excellent semiconductor properties. Through solution-processing, such as various printing methods, the fabrication of high performance CZTSSe solar cell could be applied to mass production with extremely low manufacturing cost and high yield speed. To better fulfill this goal, environmental-friendly inks/solutions are optimum for further reducing the capital investment on instrument, personnel and environmental safety. In this review, we summarized the recent development of CZTSSe thin films solar cells fabricated with benign solvents, such as water and ethanol. The disperse system can be classified to the true solution (consisting of molecules) and the colloidal suspension (consisting of nanoparticles).Three strategies for stabilization (i.e., physical method, chemical capping and self-stabilization) are proposed to prepare homogeneous and stable colloidal nanoinks. The one-pot self-stabilization method stands as an optimum route for preparing benign inks for its low impurity involvement and simple procedure. As-prepared CZTSSe inks would be deposited onto substrates to form thin films through spin-coating, spraying, electrodeposition or successive ionic layer adsorption and reaction (SILAR) method, followed by annealing in a chalcogen (S- or Se-containing) atmosphere to fabricate absorber. The efficiency of CZTSSe solar cell fabricated with benign solvents can also be enhanced by constituent adjustments, doping, surface treatments and blocking layers modifications, etc., and the deeper research will promise it a comparable performance to the non-benign CZTSSe systems.

Received June 23, 2015; accepted August 3, 2015

E-mail: jie.zhong@whut.edu.cn, jtang@hust.edu.cn

Keywords $Cu_2ZnSn(S, Se)_4$ (CZTSSe), solar cell, benign solvents, metal chalcogenide complexes (MCCs), solution processing

1 Introduction

The energy problem has drawn increasing attention because the fossil fuels are not only non-sustainable but also cause heavy pollution. It is imminent to find renewable and clean alternative energy sources to address this problem. Solar energy, a clean, easy to obtain and inexhaustible energy source, is recognized as an ideal candidate. Among various methods to exploit solar energy, the solar cell is the most feasible and effective application as it can directly convert solar energy to electricity.

$Cu_2ZnSn(S,Se)_4$ (CZTSSe) is a promising candidate as the absorber layer in thin film solar cells due to its proper band gap (1 – 1.5 eV) and high absorption coefficient (over $\sim 10^4$ cm^{-1}). Moreover, its constituents are low-cost, earth-abundant and non-toxic, which could afford massive commercial applications at low cost comparing to the more sophisticated materials such as $Cu_2InGaSe_4$ (CIGS). Various methods are used to fabricate CZTSSe which can be grouped into two categories: vacuum-based and solution-based methods. Vacuum-based methods, including sputtering [1] and co-evaporation [2], operated at strict processing conditions i.e., high temperature and vacuum, requiring expensive instruments. In contrast, solution-based methods do not necessarily need high capital investment but can yield higher efficiency, which due to the better phase and composition control associated with the solution process. Among solution-based methods, hydrazine-processing is the best in terms of conversion efficiency (12.6%) [3]. However, hydrazine is highly toxic and explosive which could restrict the widespread application of this method. Organic chemicals are another

kind of commonly used solvents, especially long-chain organic amines or acids also serving as capping agents [4]. The disadvantages of this method are that many of these organics are toxic and expensive, and often result in high carbon residues when the nano-ink films are processed into CZTSSe films, undermining the performance of CZTSSe solar cells.

To resolve these problems, CZTSSe inks with benign solvents have attracted considerable research interests. Benign solution uses water and organic solvents with low molecular weight and low toxicity (ethanol, thioglycolic acid, ammonium thioglycolate, etc.) as well as their mixture, as the dispersion media. As we know, water is the greenest and cheapest solvent. Therefore, water-based CZTSSe inks could be the optimum tends to be an environment-friendly and low-cost way to synthesize high-quality CZTSSe films.

Two more steps still need to be finished after CZTS benign inks are prepared in order to form solar cells. First, the constituent elements of CZTSSe (i.e., Cu, Zn, Sn and S/Se) are delivered to the substrate. Then, a heat treatment enables the precursor film transformed into the desired phase. The main processing steps are illustrated by following flow chart (Fig. 1).

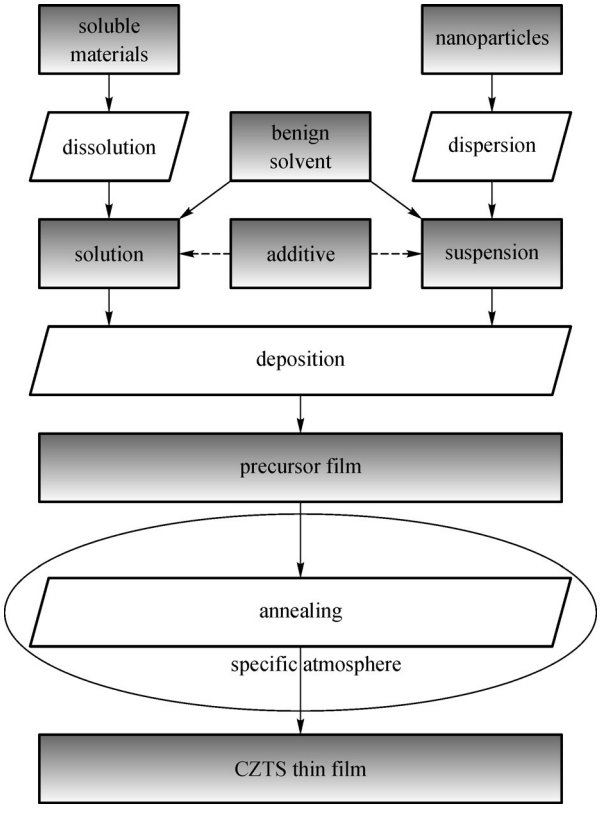

Fig. 1 Main processing steps of CZTS thin film synthesis using benign solvents

In this review, we summarize the preparation routes of benign CZTS inks and their stability mechanisms, the fabrication and chemical reactions of CZTS films, and possible strategies used to improve the performance of benign solar cells in the further research.

2 Preparation and stability of CZTS inks

2.1 Preparation methods

Generally, formation of CZTSSe inks can be grouped into two groups: true solutions and colloidal suspensions. To be more specifical, elements required for CZTS film formation are dissolved as the form of ions, molecules and/or complexes in true solutions while dispersed as nanoparticles in colloidal suspensions. These two precursors can be generally named as CZTS ink for solution processing.

2.1.1 True solutions

A large proportion of methods disperse raw materials directly into benign solvents forming solutions. Constituents of solutions are summarized in Table 1. The raw materials providing cations (Cu^+/Cu^{2+}, Zn^{2+} and Sn^{2+}/Sn^{4+}) include metal chlorides (commonly-used), metal nitrates, metal acetates and metal oxides while anions (S^{2-}) are mainly provided by thiourea (besides ammonium thioglycolate and S powder). Direct inclusion of Se^{2-} into a benign solvent seems to be very difficult. Although metal salts (chlorides, nitrates and acetates) have the best solubility, they may introduce unnecessary elements (Cl, N, C and O). When all sources are mixed, sulfur source is usually excessive in order to compensate the S loss during annealing. Water, ethanol or the mixture of them is used as solvent. In some cases, a certain additive is introduced into solutions, such as $(NH_4)_2S$ [13] and HCl (for pH adjustment [6]).

2.1.2 Colloidal suspensions

The second group of CZTSSe ink is suspensions, or called slurries. It consists of insoluble nanoparticles which are dispersed rather than dissolved in solvents. According to the composition of nanoparticles, suspensions can be classified into two groups. The one consists of intermediates (such as metal elements and sulfides) nanoparticles while the other consists of CZTS phase nanoparticles. Woo et al. [14] dispersed powder mixture of Cu, Zn, Sn and S in ethanol and proposed that there would be a reactive liquid-phase sintering between constituents when the annealing temperature exceeds the melting points of Zn (420°C) and Sn (231°C), promoting the crystallization of CZTS film. Other papers [15–18] take a preliminary reaction of the raw materials prior to mixing

Table 1 Constituents of solutions in papers

metal source	sulfur source	solvent	additive	reference
metal chlorides	thiourea	water	–	[5]
metal chlorides	thiourea	water	HCl	[6,7]
metal chlorides	thiourea	water-ethanol (30 vol% ethanol)	–	[8–10]
metal oxides	ammonium thioglycolate	water	–	[11]
metal chlorides, zinc acetate	thiourea	water	–	[12]

them into the slurries, which contains the intermediate products (oxides and sulfides). This method could remove by-products generated in the synthesis reaction, which may be detrimental to the properties of the final films [15].

Methods have also been reported to prepare CZTSSe nanoparticles to form inks. van Embden et al. has synthesized CZTS nanocrystals (NCs) that can be dispersed in benign polar solvents (such as ethanol or n-propanol), however a hot injection associated with complicated ligand exchange method was applied in the process of synthesis [19]. The hot injection routes demonstrate superiority on phase and size control and were widely applied in the non-benign solvent systems. Another commonly used method is the hydrothermal approach. The general steps of hydrothermal approach are: raw materials (such as metal chlorides and Na_2S) are added into the solvent (such as water) with a stir to dissolve them completely; the precursor mixture is transferred to a Teflonlined stainless autoclave and sealed; then autoclave containing precursor solution is kept at certain temperature for a period; after being cooled, the powders are centrifuged and washed several times to remove the impurities, by-products and unreacted raw materials. The most obvious advantage of hydrothermal method is that CZTS phase can be synthesized at a lower temperature, from 95°C to 240°C [20–28]. Several factors, including additives, sulfur source, reaction duration and reaction temperature (Table 2), can influence the products of hydrothermal method.

The CZTS produced by the hydrothermal method is shown in Fig. 2 [22]. The morphology of the particles confirmed by high-resolution transmission electron microscope (TEM) (B) and selected area electron diffraction (SAED) pattern (C), are monodispersed (A) and can be re-dispersed in ethanol forming inks (D). After the synthesis of CZTS nanoparticles, suspensions used for thin film deposition can be prepared as follows: nanoparticle powder is milled for 10 min and is then dissolved in ethylene glycol (mass ratio is 1:20) forming mixture at room temperature. After milled again for 20 min, the mixture was put under sonication for 30 min [25].

2.2 Strategies for stabilization

For the solution, it is not necessary to considerate the stability of solution when cations (Cu^{2+}/Cu^{+}, Sn^{4+}/Sn^{2+}, and Zn^{2+}) and anions S^{2-} do not coexist. This isolation of cation and anions can be achieved through either preventing the release of S^{2-} or placing cations and anions in different containers (will be further illustrated in the successive ionic layer adsorption and reaction (SILAR) approach). However, when cations and anions are mixed together, insoluble sulfide precipitates would be produced. For the suspension, nanoparticles in suspensions tend to grow up or aggregate and then precipitate, causing the instability of nanoinks. Therefore, strategies should be applied to stabilize the NCs in the inks. There are three methods were presented below.

2.2.1 Physical method

Physical method utilizes physical force, such as milling, stirring, and ultrasound, to make insoluble particles (metal elements, oxides, sulfides and synthesized CZTS NCs) dispersed in solvents. Woo et al. [14] preliminarily milled precursor powders (Cu_2S, Zn, Sn and S) to nanosize particles with large surface areas and have obtained well-dispersed slurry. Camara et al. [25] crushed synthesized CZTS nanoparticle powder for 10 min, and then milled it for 20 min with the solvent, ethylene glycol. Ultrasound as

Table 2 Factors influencing products of hydrothermally prepared CZTS NCs

	factor			
influence	additive [26]	sulfur source [28]	reaction duration [24]	reaction temperature [24]
what	phase	phase	purity	purity
how	ethylenediamine (EN) increases orthorhombic CZTS	different sulfur sources produce different phases	longer time promotes the formation of pure CZTS	higher purity at higher reaction temperature
why	EN reduces the surface energy of CZTS crystals	reaction rate of Zn^{2+} and sulfur sources determines CZTS crystal structure	complete the reaction	higher temperature provides more energy

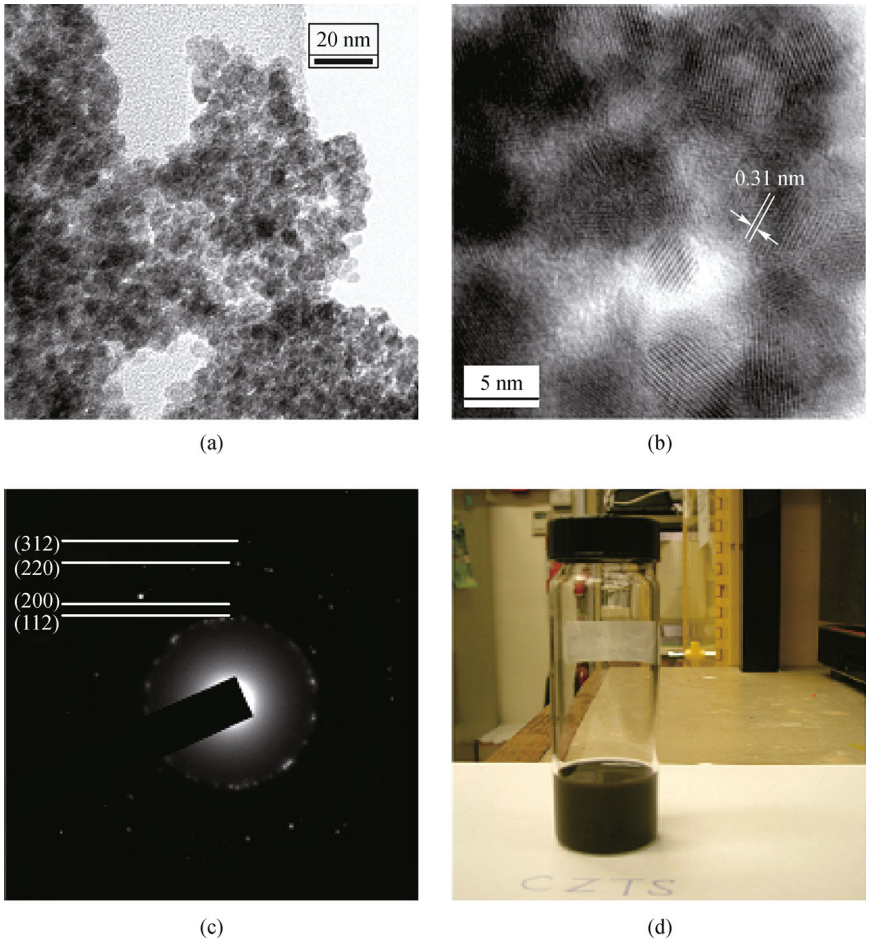

Fig. 2 TEM images of CZTS NCs prepared by hydrothermal process: (a) low resolution TEM image; (b) high resolution TEM image; (c) SAED pattern; and (d) picture of well-dispersed CZTS/ethanol 'ink' [22]

well as stirring (magnetic stirring is commonly used) are used to break the adhesion between particles in suspensions. Li et al. [17] have found the non-uniform distribution of the Cu, Zn, Sn and S precursors and relatively large precursor particles with mechanical dispersed CZTS ink. Thus, adding polymer surfactant may improve the stability of this route. However, physical method may still be neither effective nor durable in experiments for its limited stability of the inks.

2.2.2 Carbon-chain ligands capping

This method is derived from conventional hot-injection prepared nanoinks. Long chain organic molecules are used as capping agents to prevent the combination between cations and anions in the solution or prevent the aggregation of nanoparticles in the suspension. Zhao et al. [29] prepared hydrophilic CZTS NCs in aqueous solutions using thioglycolic acid as the stabilizer and the hydrophilicity enabled the NCs good dispersion in water. Ethylenediamine as the chelating agent was added to the solution consisting of metal salts and sulfur source for hydrothermal synthesis [22]. The strong coordination ability of organic thiols with metal ions enabled metal oxides to be dissolved in the aqueous solution with ammonium thioglycolate [11]. Tian et al. employed PVP as the ligand to obtain CZTS nanoinks without obvious aggregation. Metal sulfides were dispersed homogenously in either water or ethanol with the capping of (*n*-hexadecyl) cetyltrimethyl ammonium bromide(CTAB) (Fig. 3) [17].

Despite high stability brought by carbon ligands, the low conductivities of CZTS films were caused by the phase separation and low crystallization. The impurities from organics residues remain at the interface may act as the carriers recombination centers. And high annealing temperature is necessary in order to promote the CZTS crystallization.

2.2.3 Self-stabilization

Metal chalcogenide complexes (MCCs), described as a kind of novel inorganic ligand, can effectively replace the carbon-chain ligands [30–33]. Kovalenko et al. [30,31]

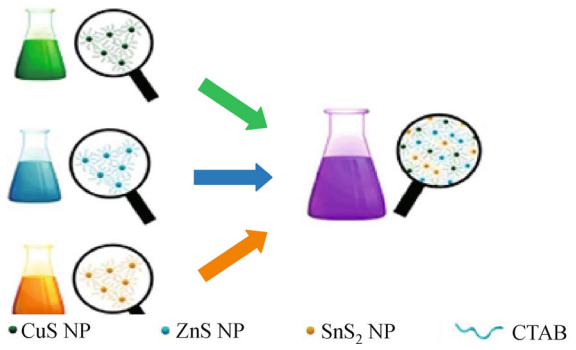

Fig. 3 Schematic diagram of the preparation of CZTS solution using metal sulfides with cetyltrimethyl ammonium bromide (CTAB) as the capping ligand. A typical illustration of carbon-chained ligands capping on the NCs [17]

used hydrazine processed $Sn_2S_6^{4-}$ as MCC to cap CdSe NC_s and they discovered that CdSe NCs can be capped with various MCCs. Jiang et al. [32] and Zhou et al. [33] have utilized this method to fabricate CZTS nanoinks, however they used non-benign hydrazine or organic solvents (such as *N*-methylformamide [32]) as the solvents and tedious ligands exchanging as the capping method.

In our past work, we have proposed a novel and effective strategy, namely self-stabilization, to prepare benign CZTS nano ink [13]. We specifically designed a route to prepare aqueous Sn-MCCs ($Sn_2S_6^{4-}$ and $Sn_2S_7^{6-}$) using metallic Sn power and S with $(NH_4)_2S$ aqueous solution. When Cu^{2+}/Zn^{2+} solutions were blended to the previous solution, Cu/Zn sulfide NCs were formed and instantaneously capped by the Sn-MCCs rather than precipitating. And these MCC ligands can deter metal sulfides from growing and keep the long-term stability (over 6 months in ambient conditions). Figure 4 illustrates the process of synthesis of self-stabilized ink. This route realizes an instant self-component capping in an one-pot technique, and no further exchanging, wash, separation steps are required.

The characterizations of CZTS nanoinks were shown in Fig. 5 [13]. Raman spectrum (Fig. 5(b)) detected that Sn-MCCs solution contained $Sn_2S_6^{4-}$ (280, 344, 367 cm^{-1}) and $Sn_2S_7^{6-}$ (300, 351 cm^{-1}). The S-Sn (1000 – 1200, 1400 cm^{-1}) vibration both existed in the vacuum-dried CZTS inks and the precipitation from centrifugation (Fig. 5(c)), suggesting Sn-MCC_s were coated on the precipitated NCs. The Zeta-potential in nanoinks was –39.8 mV, which provided a strong binding between negative $Sn_2S_6^{4-}$/$Sn_2S_7^{6-}$ and NC_s. The good stability and homogeneity enable this nanoink to be applied in different types of deposition techniques, such as spin coating, inject printing, spray printing.

3 Fabrication of CZTS films

3.1 Deposition techniques

We summarized four film deposition techniques which were commonly used in CZTSSe film preparation: spin-coating, spraying, electrodepositon, and successive ionic layer adsorption and reaction (SILAR). They demonstrate different advantages and shortages which could serve for various aims.

3.1.1 Spin-coating

Spin-coating is a common technique for liquid deposition in laboratories due to its high reproducibility and suitability for various solutions. Thus, many researchers made CZTS thin films through spin-coating [8–11,13,34]. It is notable that a large proportion of precursor solutions used in this technique were sol-gel [8–10,34]. Sol-gel owned three main merits [34]. First, elemental constituents can be uniformly blended on a molecular level, which can accelerate the reaction and facilitate the formation of homogeneous phase. Second, thin films can crystallize under a lower annealing temperature because nanoparticles constitute the gel. Third, controlled extrinsic doping can be easily achieved due to its good mixture.

However, the drawbacks of spin-coating method were also obvious. Spin-coating process should be repeated several times in order to get proper thick thin films (summarized from above papers). This process could cost much more time when the solid concentration of CZTS ink was low. Considerable volumes of the solution dropped on the substrate surface were spun off, resulting in the low

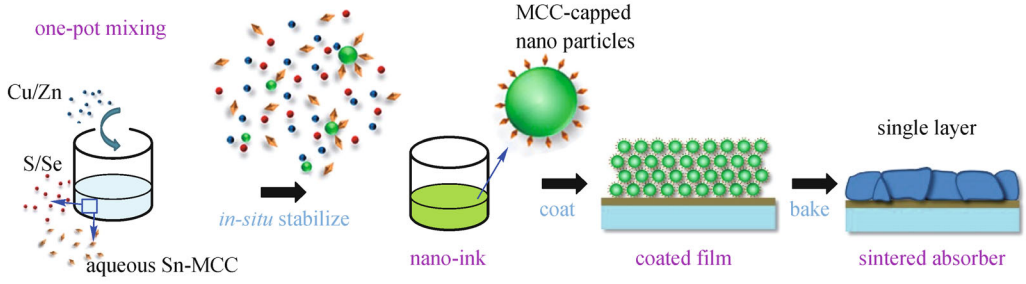

Fig. 4 Schematic diagram of the self-stabilized ink [13]

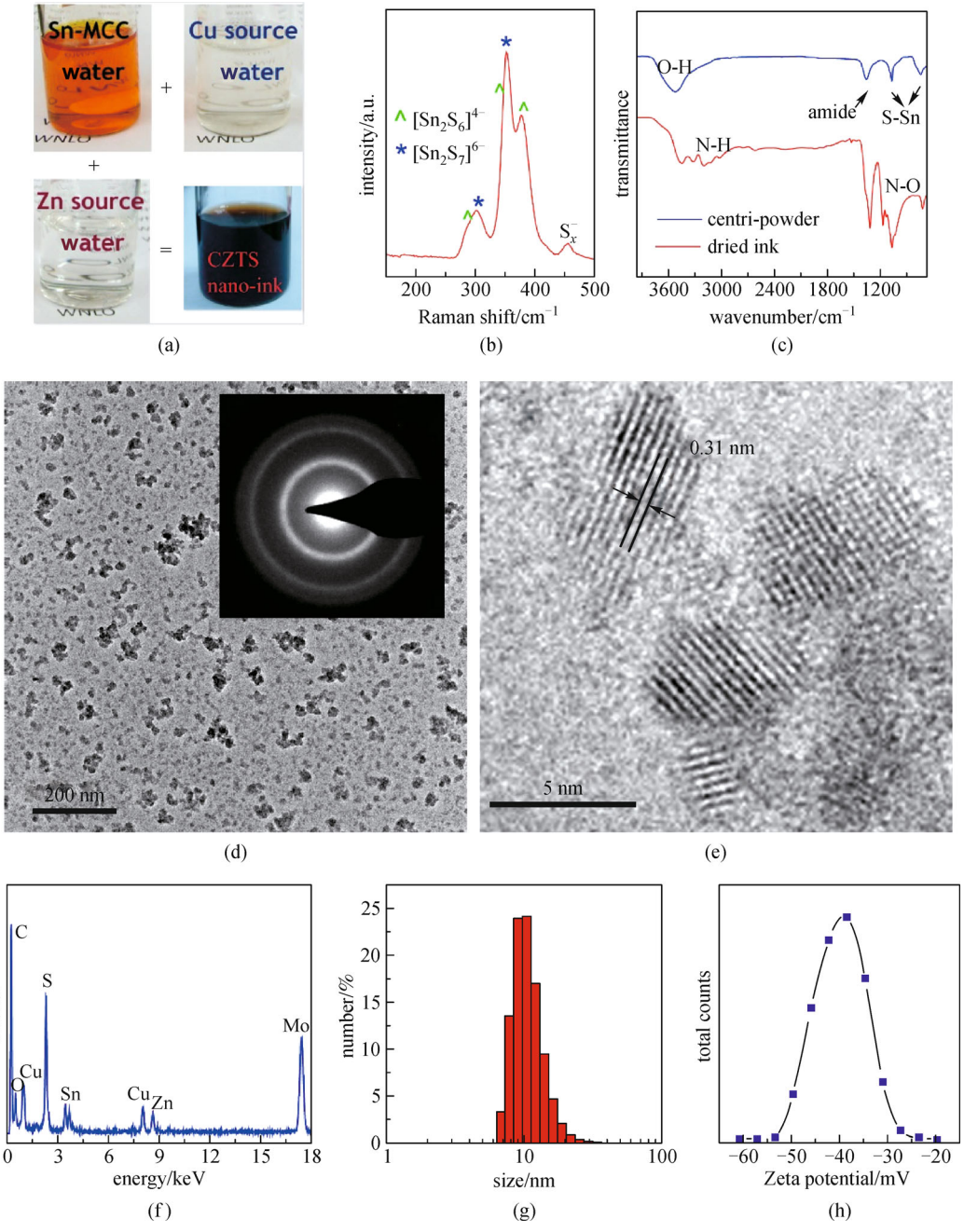

Fig. 5 CZTS nanoinks preparation and characterization. (a) Photos of CZTS nanoinks processed by one-pot mixing of aqueous Sn-MCC and Cu/Zn sources; (b) Raman spectrum of aqueous Sn-MCC solution; (c) FTIR spectra of CZTS inks vacuum-dried (dried ink) and the precipitation from centrifugation (centri-powder); (d) TEM morphology of the dispersed NCs with the SAD pattern; (e) high-resolution TEM image of a few NCs with measured lattice distance of 0.31nm corresponding to the (111) lattice distance of Cu/ZnS; (f) EDS analysis of as-made CZTS NCs. A Mo grid with carbon support film was used to manifest that the Cu signal is from NCs; (g) DLS characterization of the CZTS nanoink; (h) Zeta-potential curve of aqueous nanoink associated with MCC capping [13]

material utilization. Moreover, this route is also restricted from large area preparation.

3.1.2 Spray deposition

Spray-related technique is a widely used deposition method not only in laboratories but also in our daily life. An aerosol from the precursor solution is delivered to the substrate surface through a carrier gas, such as compressed air [12], argon [7] and nitrogen [15]. This technique can be further divided into two groups: the pyrolysis technique [5–7,12,35] and the non-pyrolytic technique [15–17]. Traditional pyrolysis technique adds all element sources into the solvent and then sprays the solution to the substrate

directly, ending up reaction under heating. These reactions would release some by-products which tend to damage the performances of the device [15,35].

Larramona et al. [15,16] first synthesized the Cu-Zn-Sn-S colloid and then washed it, re-dispersing the residual nanoparticles to make an ink which would be sprayed to the substrate. However, the CZTS films made by this method tended to be more porous than the pyrolysis technique, which would increase the surface area resulting in fast surface oxidation [15]. Moreover, the considerable secondary phases, ZnS grains, remained in the final device (Fig. 6 [15,16]). Li et al. [17] initially synthesized binary sulfide (i.e., CuS, ZnS and SnS_2) and then mixed these sulfide nanoparticles in the ratio 2:1:1 in water or ethanol. The sulfide particles would react on the surface after being sprayed to the substrate, forming quaternary compound CZTS.

For spray deposition, the substrate temperature is a key that it can influence both the morphology and the stoichiometry of the CZTS film [5,7]. A possible disadvantage of sprayed CZTS is its roughness could cause carriers combination at CZTS/CdS interface [7].

3.1.3 Electrodeposition

Electrodeposition is suitable for large-area coating with high materials utilization (up to 90%) [36]. Two electrochemical methods have been used to deposition CZTS films: the stacked elemental layer (SEL) approach [36–39] and the co-electrodeposition approach [40–44]. The SEL approach electrodeposits metals one-by-one to make a stacked precursor film and this precursor is sulfurized in either elemental S vapor or H_2S (the latter is confirmed to be more effective at converting the precursor in to CZTS [39]). The other approach co-electrodeposits metal as an alloy or even provides all constituents including S from the same electrolyte [43]. Also, sequent anneal is necessary to make a compact film.

Overall, the electrodeposition approach has high utilization especially for industrial production. Nevertheless, it is complicated compared with spin-coating and spray. In some cases, additives (sorbitol [36], methane sulfonic acid [36], sodium-pyrophosphate [41], etc.) are added as supporting electrolyte which can result in impurities and toxins involving. For aqueous solutions, a

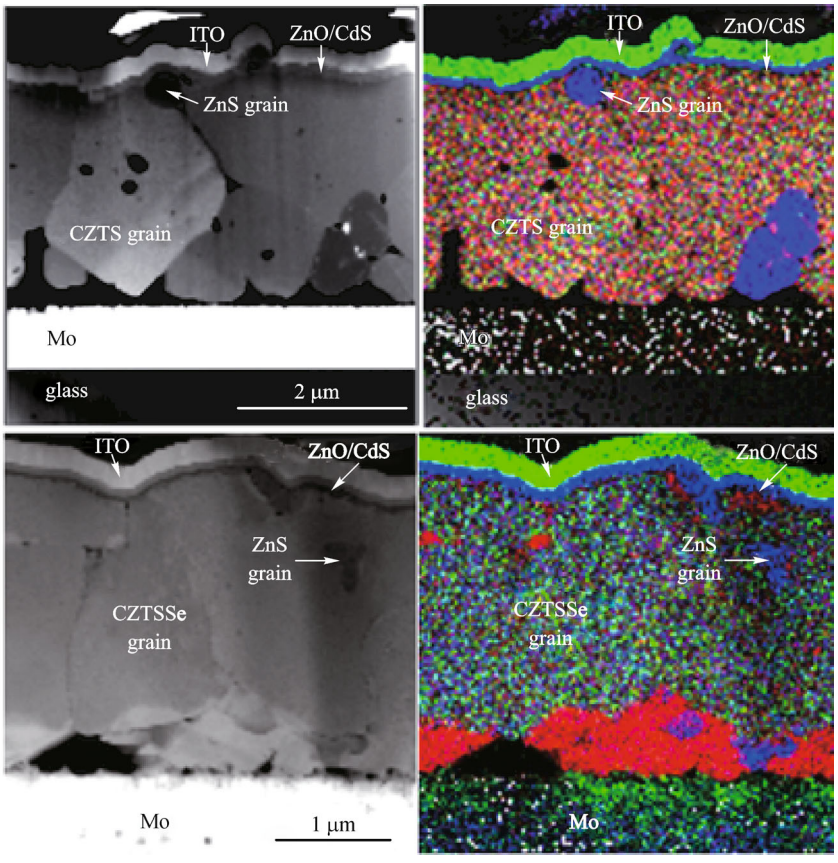

Fig. 6 Dark-field STEM image and corresponding EDX-STEM mapping for Cu, Zn, and Sn elements in a slice of a Mo/CZTS (Se)/CdS/ZnO/ITO device (Cu: red, Zn: blue, Sn: green) with a CZTS (Se) film made by non-pyrolytic spray [15,16]

massive hydrogen evolution happens at the working electrode resulting in hydrogen embitterment [45].

3.1.4 SILAR

The dispersions of the solutions used in the SILAR method [46–50] are ions and cations as well as anions are deposited separately. Figure 7 [48] illustrates the procedure of SILAR technique and its growth mechanism is [50]: (1) cations are absorbed onto the substrate forming Helmholtz Electric Double Layer; (2) loosely bounded cations are rinsed; (3) anions are absorbed from anionic solution and react with the cations; (4) excess and unreacted species are rinsed. By repeating this cycle, the proper thickness can be obtained.

The thin film can be deposited only through immersing. This simplicity provides the feasibility for large-scale production. It is the deposition cycles and time that are used to adjust the thickness of SILAR method. Finally, this technique has less strict requirements for the substrate materials, which expands the range of application of SILAR method [49]. For instance, deposit CZTS onto glass, stainless steel and fluorine doped tin oxide (FTO) substrate respectively.

Imitating SILAR approach, several derivative methods are invented. Su et al. [51] and Gao et al. [52] deposited Cu_2SnS_x and ZnS sequentially involving SILAR and then the stacked layer precursor film was annealed to synthesize CZTS. Wangperawong et al. [53] deposited SnS and ZnS in sequence through chemical bath deposition (CBD). After that, ion exchange was used to incorporate copper to form final CZTS.

Table 3 summarizes the main features of the four deposition techniques. Although these techniques are the commonly-used methods to transform benign solutions into CZTS thin films, there are still other approaches, consisting of doctor blading [18,29], photo-chemical deposition [54] and chemical bath deposition [55].

3.2 Annealing

To form a compact and homogenous CZTS thin film and fabricate CZTSSe solar cells, an annealing step is indispensable. Theoretically and empirically, a high-quality CZTS thin film should be nearly stoichiometric (the copper-poor and zinc-rich CZTS is generally regarded as a good film [56]) without harmful secondary phases and impurities. The elimination of impurities should be carried

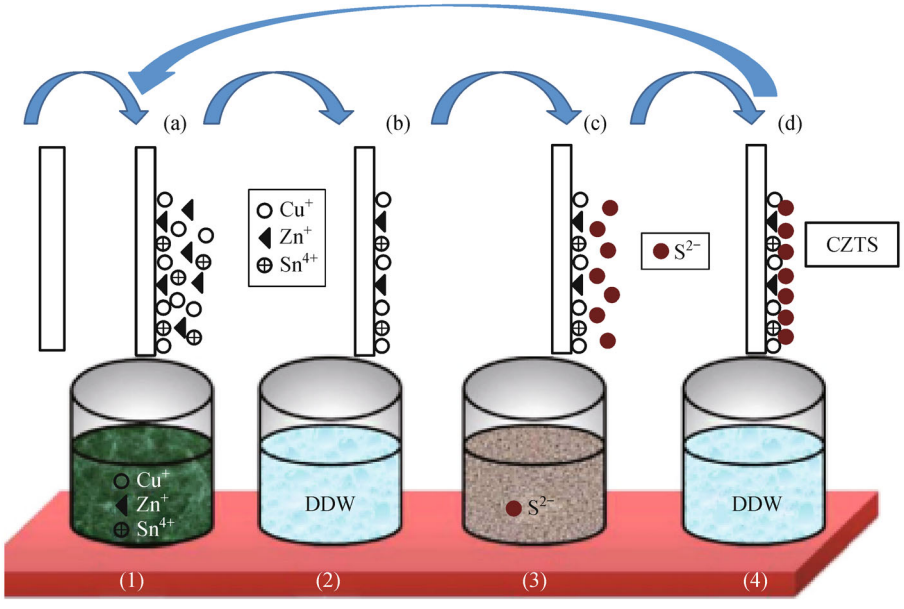

Fig. 7 Schematic diagram of SILAR technique for the deposition of CZTS: beaker 1 contains cationic precursors, beaker 3 contains anionic precursor and beakers 2 and 4 contain double distilled water (DDW) [48]

Table 3 Comparison of different deposition techniques with highest efficiencies

techniques	time-consuming	simplicity	large-scale production	solution/ suspension	quality of film	highest efficiency
spincoating [11]	no	yes	no	both	general	6.62%
spray [16]	no	yes	yes	both	general	8.60%
electrodeposition [41]	no	no	yes	solution	good	3.40%
SILAR [46]	yes	yes	yes	solution	general	1.85%

out carefully in every step considering that the performance of solar cells is extremely sensitive to impurities. In terms of raw materials, elements and sulfides are better than salts (anions could be the unwanted elements) while oxides (the oxygen is too stable to be removed) are the worst. In the annealing process, inert gases or chalcogenide vapors are introduced to prevent impurities from the air.

The first process of annealing is that solvents (such as water and ethanol) and volatile organic additives (if any, such as ethanediamine and thioacetamide) will volatilize, or decompose into smaller molecules and then volatilize. When temperature is increased to a higher and stable level, CZTS crystals start to be formed. But the formation process is different for films deposited by different methods or from different solutions illustrated in Table 4. Using inks consisting of CZTS nanoparticles made by hydrothermal method, the kesterite nanoparticles would grow up due to the mutual annexing. In terms of orthorhombic and wurtzite nanoparticles, as they are metastable while kesterite phase is stable, annealing process would transform it into kesterite phase [20,26,28]. Jiang et al. [26] figured out that the transformation temperature from the orthorhombic structure to the kesterite structure was 500°C. Tiong et al. [28] discovered that a part of wurtzite CZTS decomposed into Cu_3SnS_4 during thermal treatment.

When metal sources and sulfur source both exist in solution or they are both deposited on the surface of substrates, the reactions take place among metal sulfides [57,58]. The extent of crystallinity of CZTS increases with annealing temperature as shown in Fig. 8 [8]. The precursor films made up of oxides or electrodeposited stacked metallic layers without S would be sulfurized with S or H_2S [18,39,44].

In our previous work [13], the CZTS thin film spin coated on molybdenum-coated soda-lime glass was baked in a glove box filled with nitrogen. The coating and heat treating (180°C and 400°C) process were repeated ten times for a targeted absorber thickness. In a glove box full of nitrogen, with 5 – 50 mg addition of selenium to tune the band gap of absorber, the final annealing (540°C – 600°C, 10 – 25 min) was carried out in a covered hot-plate, obtaining CZTSSe film. The characterization of CZTSSe film is shown in Fig. 9. The Raman curves (Fig. 9(a)) and XRD pattern (Fig. 9(b)) illustrated the composition of the thin film can be gradually changed from CZTS to CZTSe with the increase of Se ratio. The cross-sectional (Fig. 9(c)) and top-view (Fig. 9(d)) SEM images confirmed the absence of impurity and obvious crack in CZTSSe layer. The solar cell achieved the photoelectric conversion efficiency of 5.14% (Fig. 10(a)) whose absorber was the annealed CZTSSe thin film with 1.22 eV band gap (Fig. 10 (b)).

4 Optimization

We also review some papers that propose optimization strategies to achieve either a high-quality CZTS thin film or a high-efficiency solar cell. These approaches can be similarly applied to optimize the CZTSSe thin film solar cell fabricated by benign solution [59–61].

4.1 Optimal compositional ratios

It is well known that the compositional ratios $Cu/(Zn + Sn) \approx 0.85$ and $Zn/Sn \approx 1.25$ are optimal for high efficiencies [59]. Two dominant advantages can be brought from the Cu-poor and Zn-rich composition. First, according to the calculation of Chen et al. [62], this condition will promote the formation of Cu vacancy (V_{Cu}) while suppress the formation of the donor defect Cu_{Zn} antisite. The Cu_{Zn} is more effective to be the recombination center, which is detrimental to the performance of CZTS solar cell, because its level is deeper than V_{Cu}. Thereby, the Cu-poor and Zn-rich condition is beneficial.

Second, on the basis of the relation between different secondary phases formation and the ratios of $Cu/(Zn + Sn)$ and Zn/Sn reported by Vigil-Galán et al. [63], their formation will be inhibited when the compositional ratios reach the optimum. The ZnS binary phase existed in all cases while the Cu_2SnS_3 (CTS) ternary phase disappeared in Zn-rich ones. Nevertheless, their appearances were both restrained in the Cu-poor and Zn-rich circumstance. As for the CuS phase, its volume arised with the augment of $Cu/(Zn + Sn)$ ratios (between the range of 0.80 and 1.01).

Table 4 Comparison of annealing conditions for CZTS film deposited using different techniques

components	solution/ suspension	deposition technique	temperature/°C	time/min	atmosphere	reaction
Cu_2S + metal elements [14]	suspension	spin-coating	400 – 530	30	$N_2 + H_2S$ (5%)	liquid phase sintering
metal sulfides [52]	solution	SILAR	200 – 500	120	$N_2 + S$	solid state reaction
metal oxides [18]	suspension	doctor-blading	250 – 600	30	S	sulfuration
metastable CZTS [28]	suspension	doctor-blading	550 – 600	30	S	phase transformation (to kesterite)
kesterite CZTS [25]	suspension	spin-coating	450	60	N_2	growth
metal sulfides [13]	suspension	spin-coating	540 – 600	10-15	$N_2 + Se$	solid state reaction

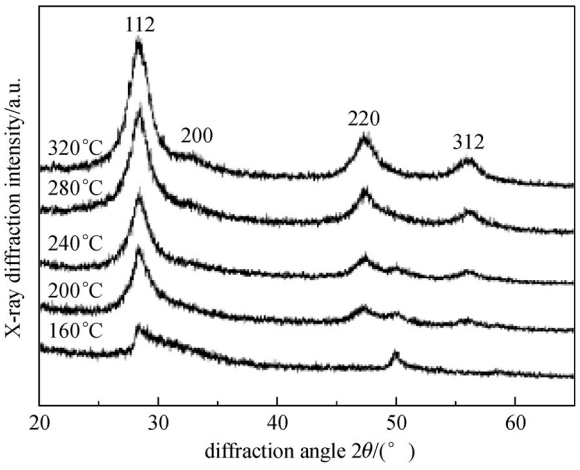

Fig. 8 XRD patterns of CZTS thin films as a function of annealing temperatures [8]

However, the efficiencies of solar cells using CZTS thin films as absorbers increased when the values of Cu/(Zn + Sn) ratios decreased. Therefore, the performance will be enhanced in Cu-poor and Zn-rich conditions resulting from the inhibition of secondary phases formation. Interestingly, all secondary phases were found in the near stoichiometric sample, i.e., Cu/(Zn + Sn) = 1.01 and Zn/Sn = 0.98.

Various measures can be taken to adjust the elemental composition of CZTS to obtain the optimum. Vigil-Galán et al. also [7] have investigated this problem in detail when they fabricated CZTS thin film through spray pyrolysis. Table 5 shows the influence of several different conditions on the composition of CZTS thin film with the dectection of X-ray fluorescence (XRF). From this table, we can learn that the elemental ratios in solution (stoichiometry or nonstoichiometry), the composition of annealing atmosphere and chemical etching all affect the compositional ratios. These factors are universal for all solution-based methods not only effective for the spray pyrolysis technique.

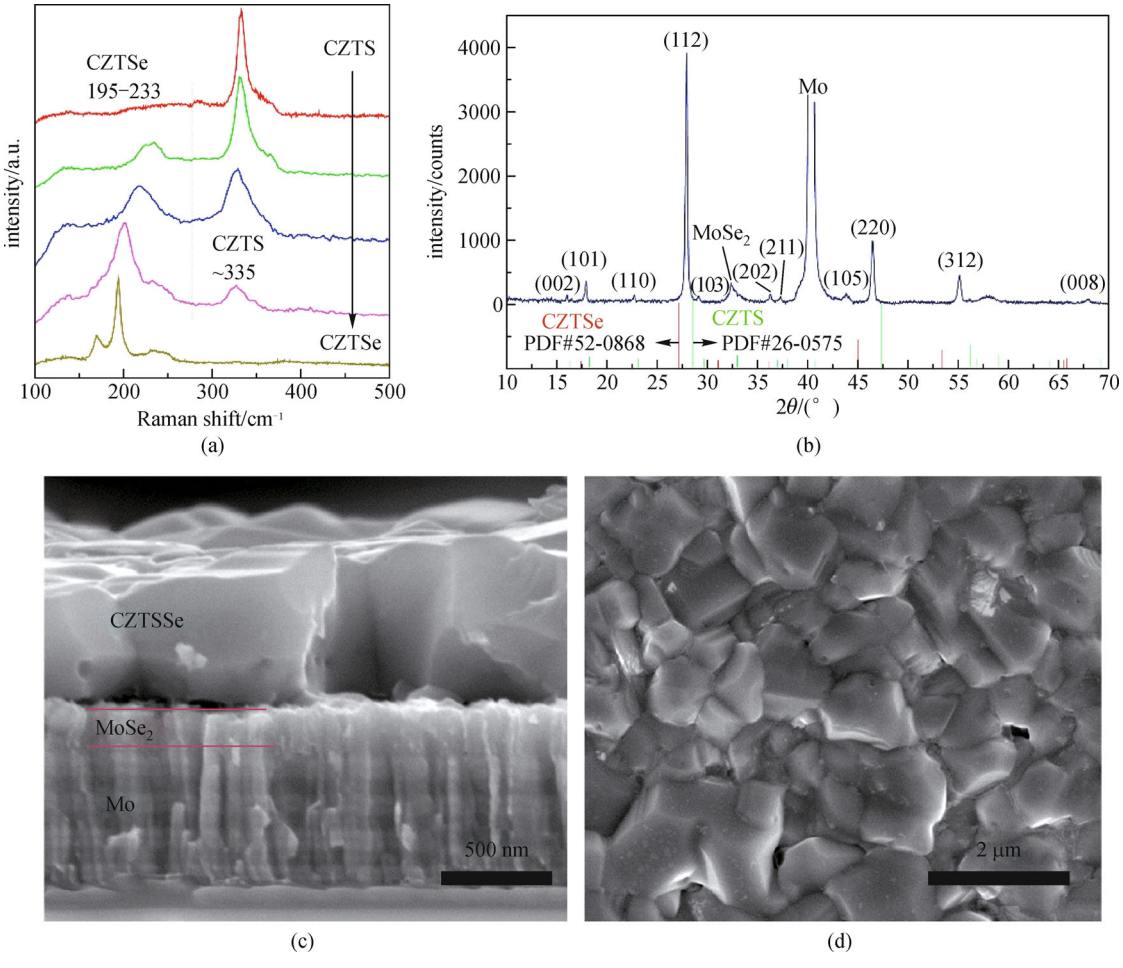

Fig. 9 Characterization of CZTSSe film. (a) Raman curves of the CZTSSe film produced by annealing the CZTS film in an atmosphere containing different amounts of Se and S, indicating a fully tunable composition and consequently a band gap; (b) XRD pattern of the CZTSSe absorber film. Peaks indexed to Mo and $MoSe_2$ (from substrate) as well as the standard diffraction patterns for CZTS (JSPDS 26-0575) and CZTSe (JSPDS 52-0868) are included for reference; (c) cross-sectional and (d) top-view SEM images of the CZTSSe absorber film [13]

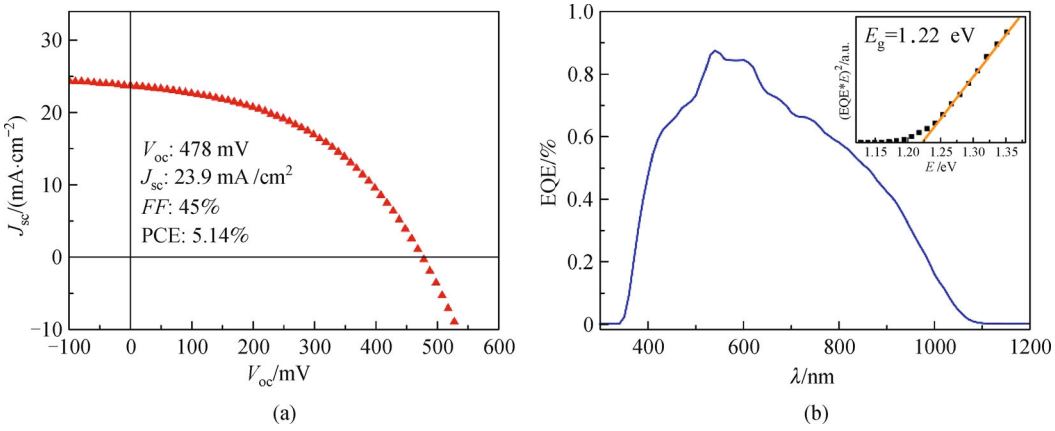

Fig. 10 (a) *J-V* curve and (b) EQE spectrum of the CZTSSe device fabricated from aqueous CZTS nanoink [13]

Table 5 Compositional ratios of the precursor elements for as-deposited, annealed, and annealed and chemically treated samples. The as-deposited samples were deposited from stoichiometry and nonstoichiometry solutions [7]

samples	Cu/(Zn + Sn)	Zn/Sn
As-deposited (from stoichiometry solution)	0.96	0.79
annealing with S (550°C) (from stoichiometry solution)	1.01	0.98
annealing with S (550°C) + KCN (from stoichiometry solution)	0.58	0.90
annealing with S + Sn (550°C) (from stoichiometry solution)	0.99	0.92
annealing with S + Sn (550°C) + KCN (from stoichiometry solution)	0.52	0.94
As-deposited (from nonstoichiometry solution) (−20% Cu and +20% Zn)	1.00	1.13
annealing with S + Sn (550°C) (from nonstoichiometry solution) (−20% Cu and +20% Zn)	0.80	1.37

Besides, there are other specific factors influencing the elemental constituent of CZTS thin film deposited by different approaches, such as the substrate temperature (spray deposition) [7], plating time (electrodeposition) [37] and immersing time (SILAR) [53]. However, the influence of these factors is seemingly hard to be controlled accurately and thus needs exploration in the specific experiment.

4.2 Doping

The poor crystallization, such as small grain and non-compact morphology, boosts the increase of Rs and the recombination of the photocurrent [34]. The crystallinity of CZTS with Na-doping demonstrates sharper XRD peaks, indicating better crystallinity or larger grain sizes of Na doped CZTS films [34]. This result is confirmed by Wen et al. [64] and Prabhakar & Jampana [65]. Tong et al. [66] and Johnson et al. [67] find another alkali metal, potassium (K), is also beneficial for the growth of grains. Therefore, in order to improve the crystallinity, Na/K-doping is a feasible and convenient method for CZTS thin films from solution as these elements can be easily doped into solutions.

The function of Na-doping is more than improvement of crystallization. The electrical properties of CZTS thin films are enhanced significantly. Zhou et al. [68] fabricated the solar cell based on CZTS:Na nanocrystals and its SEM image is shown in Fig. 11(a). They measured the electrical characterization of the CZTS:Na- and CZTS- based devices. Figures 11(b) and 11(c) show that open circuit voltage (V_{oc}), short circuit current (J_{sc}), fill factor (*FF*) and external quantum efficiencies (EQE) all have been enhanced when CZTS was substituted by CZTS:Na as the absorber layer. Devices with Na-doping CZTS absorber also have longer minority carrier lifetime and higher carrier concentration: the minority carrier lifetime of CZTS:Na- and CZTS- based solar cells are 3.6 and 1.5 ns, respectively, characterized by time-resolved photoluminescence (TRPL) as shown in Fig. 11(d); the carrier densities are (9 – 10) and (8 – 9) × 10^{15} cm^{-3} for the CZTS:Na- and CZTS-based devices, respectively, measured by capacitance-voltage (*C-V*) test as shown in Fig. 11(e). The improvement of electrical properties attributes to the effective defect passivation of Na-doping and leads to 50% enhancement of power conversion efficiency (PCE) (increased from 4% to 6%). Wen et al. [64] and Nagaoka et al. [69] also observed the conductivity and hole concentration can be enhanced through Na-doping. The improvement of the electrical properties is explained by that Na

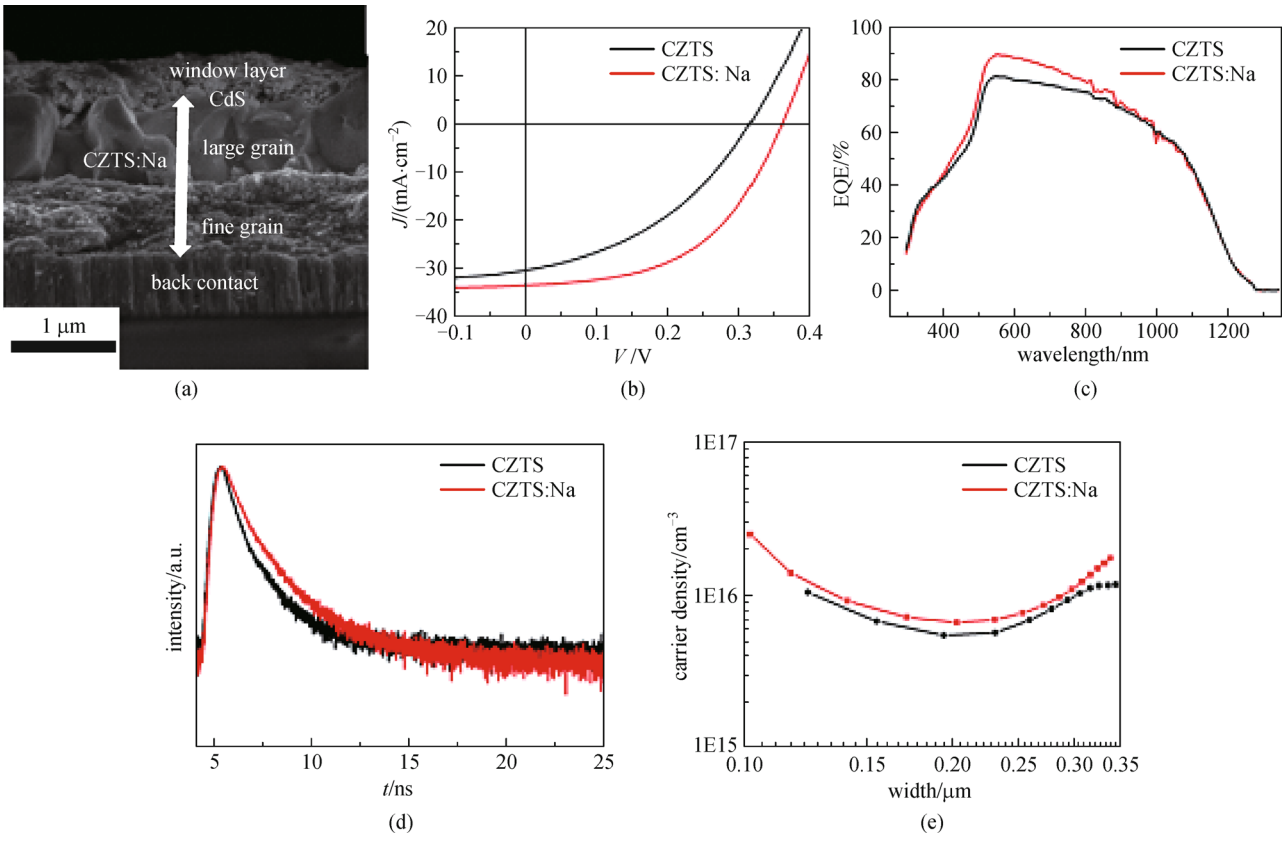

Fig. 11 (a) SEM image of typical solar cell based on CZTS:Na nanocrystals. Electrical characterization of the CZTS:Na- and CZTS-based devices; (b) current-voltage (J-V) characteristics under air mass 1.5 illumination, 100 mW/cm^2; (c) EQE spectrum of the device without any applied bias; (d) TRPL of the device under low injection; (e) capacitance–voltage measurement, with the measurement frequency of 11 kHz, the DC bias ranging from 0 to − 0.5 V, and the temperature at 300 K [68]

tends to aggregate at the grain boundaries where defects also aggregate. These defects resulting in the recombination of photo-excited electron and hole are passivated by Na and thus the performance is enhanced [70].

4.3 Surface treatments

The surface composition of CZTS film is crucial for the device performance because it affects the defects in the depletion zone where photo generated carriers generate and separate. Secondary phases (metal sulfides) can be the unwanted composition and these phases can be removed by surface etching. For example, aqueous KCN can be used to remove copper sulfide phases [36]. In our previous work [71], we have researched the relation of the surface compositions to bulk defect depths and doping densities in detail.

As-deposited CZTSSe thin films were annealed in sulfur vapor but the sulfur content was varied to obtain different samples. Sample S1 (below 1 mg S) had no efficiency while sample S2 (4 mg S) and sample S3 (6 mg S) had the efficiencies of 1.16% and 6.4%, respectively. Through Auger electron spectroscopy (AES) depth analysis, we observed that remarkable elemental variations appeared at the surfaces (within 250 nm) while the elemental ratios over 250 nm were homogenous and close among three samples. The surface composition of S1 was copper-rich, resulting in short circuiting. In contrast, S2 and S3 were copper-poor at surfaces.

However, the reason that made the efficiency of S3 exceed that of S2 significantly was unknown, yet. Thereby, Admittance spectroscopy (AS) characterization was used to estimate the energy level of defects. Capacitance-frequency (C-F) scans for S2 and S3 are shown in Figs. 12 (a) and 12(b), respectively. The C_m curve of S2 (Fig. 12(a)) slumps at around 10^5 Hz whereas the sharp drop of S3 (Fig. 12(b)) happens at 10^6 Hz. According to Walter's theory [72], it can be asserted that the defect levels of sample S2 is deeper than S3. This assertion is confirmed by the phenomenon that S3 reaches the peak at higher frequency region than S2, in the trap conductance spectra $(G_m - G_d)/\omega$ (Fig. 12(c)). The actual energetic depths of the defect (E_a) for S3 and S2 are 101 and 156 meV, respectively, estimated by linearly fit Arrhenius plots (Fig. 12(d)). The deep trap and large E_a are the character of the effective recombination center, which hurts the performance of S2.

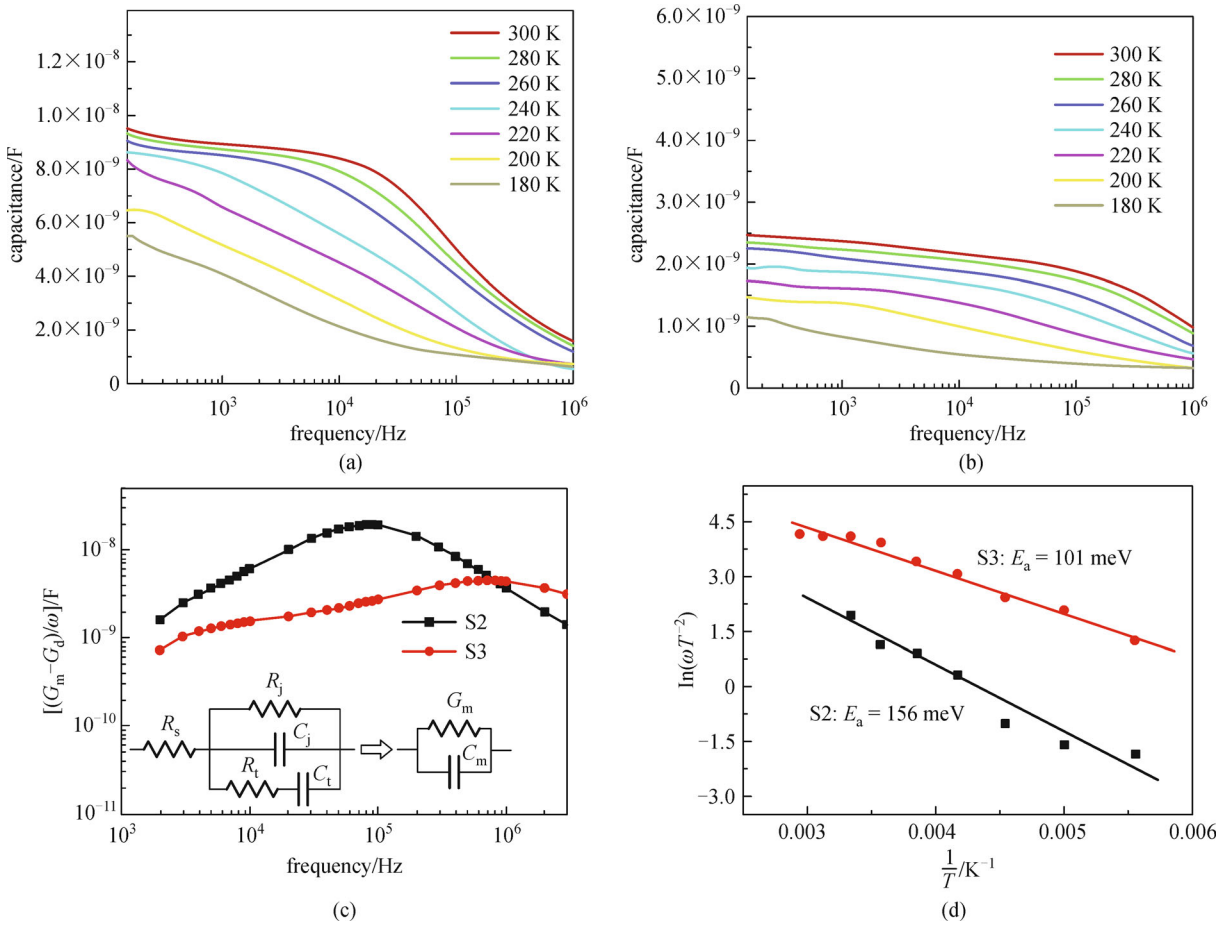

Fig. 12 Electronic characterization for CZTSSe devices S2 and S3. Admittance spectroscopy (AS) of S2 (a) and S3 (b) with temperature range of 180 to 300 K; (c) the trap conductance spectra $(G_m-G_d)/\omega$; and equivalent circuit model; (d) Arrhenius plots of S3 and S2 derived from AS patterns. The estimated energetic depths of the defect (E_a) for S3 and S2 are 101 and 156 meV, respectively [71]

Moreover, S3 (9.7×10^{15} cm^{-3}) possesses the lower calculated p-type doping density than S2 (1.1×10^{17} cm^{-3}) from capacitance-voltage (*C-V*) characterization. Therefore, it is the type and density of defect at surfaces caused by different sulfurization process that determine the photovoltaic performances to a large extent.

In view of the above analysis, we have proposed a simple and effective sulfurization process (at about 10 kPa sulfur pressure) to manage the surface reaction as well as the diffusion of Cu, Zn and Sn, optimizing the surface constitution.

4.4 Back contact blocking layers

Even if a high-quality CZTS thin film might be synthesized though above optimizations, some challenges still hinder the manufacture of high-efficiency solar cells. Traditionally, CZTS thin films are deposited on the surface of Mo glass and the formation of MoS_2 or $MoSe_2$ is inevitable. On the one hand, adequate thin MoS_2 or $MoSe_2$ is beneficial for the solar cell due to the quasi-ohmic contact and good adhesion with the CZTS film [59,73]. On the other hand, the thick MoS_2 or $MoSe_2$ layer contribute to high series resistance [73]. Thin barrier layers, such as Ag [74], ZnO [75], and TiN [76], are introduced to inhibit the side reaction. Although the barrier layer currently degrades the crystallinity of the absorber lowering V_{oc}, it improves the efficiency by enhancing J_{sc} and *FF* [77].

5 Conclusions

Constituent materials of CZTS can be dissolved or dispersed in benign solvents (such as water and ethanol) according to their solubility. The stability of the benign solution is critical and three strategies are come up with. Physical milling is simple, but it still requires organic chemicals to maintain certain stability. Chemical capping method is effective but can lower the conductivity of the thin film and includes impurities as organics are introduced. The self-stabilization route with aqueous system seems to be an excellent strategy in terms of its high

availability and long durability without introduction of unwanted carbon chains. Various coating techniques are applied to deposit CZTS films. Spin-coating is easy to implement but not suitable for large-scale production; spray method can be applied to almost any kind solution/suspension; electrodeposition outputs the high quality film but the process is complicated; SILAR can be operated simply but consumes a large amount of time.

The efficiency of the CZTS solar cell prepared by benign solution process is not as high as non-benign cousin. Given the merits of that benign solution processing is an environment-friendly, low-cost, and high-utilization approach for large-scale synthesis of CZTS thin films, more research efforts are worthy to be devoted to this area. It is necessary to note that the self-stabilization route with aqueous media has demonstrated very competitive strength in both production-cost and film qualities among benign CZTS inks. Integrated with roll-to-roll printing process, the CZTS solar cells can be "real" low cost and environmentally friendly in both aspects of materials and fabrication.

Acknowledgements This work was financially supported by the National Natural Science Foundation of China (NSFC) (Grant Nos. 61274055 and 61322401), China Postdoctoral Science Foundation (No. 2013M542015) and Fundamental Research Funds for the Central Universities, Huazhong University of Science and Technology (No. CXY12M008). Jie Zhong acknowledges the support of Foundation for Scientific Research of Wuhan University of Technology.

References

1. Katagiri H, Jimbo K, Yamada S, Kamimura T, Maw W S, Fukano T, Ito T, Motohiro T. Enhanced conversion efficiencies of Cu_2ZnSnS_4-based thin film solar cells by using preferential etching technique. Applied Physics Express, 2008, 1(4): 041201
2. Schubert B A, Marsen B, Cinque S, Unold T, Klenk R, Schorr S, Schock H W. Cu_2ZnSnS_4 thin film solar cells by fast coevaporation. Progress in Photovoltaics: Research and Applications, 2011, 19(1): 93–96
3. Wang W, Winkler M T, Gunawan O, Gokmen T, Todorov T K, Zhu Y, Mitzi D B. Device characteristics of CZTSSe thin-film solar cells with 12.6% efficiency. Advanced Energy Materials, 2014, 4(7): doi: 10.1002/aenm.201301465
4. Zhang H, Hu B, Sun L, Hovden R, Wise F W, Muller D A, Robinson R D. Surfactant ligand removal and rational fabrication of inorganically connected quantum dots. Nano Letters, 2011, 11 (12): 5356–5361
5. Kamoun N, Bouzouita H, Rezig B. Fabrication and characterization of Cu_2ZnSnS_4 thin films deposited by spray pyrolysis technique. Thin Solid Films, 2007, 515(15): 5949–5952
6. Zeng X, Tai K F, Zhang T, Ho C W J, Chen X, Huan A, Sum T C, Wong L H. $Cu_2ZnSn(S,Se)_4$ kesterite solar cell with 5.1% efficiency using spray pyrolysis of aqueous precursor solution followed by selenization. Solar Energy Materials and Solar Cells, 2014, 124: 55–60
7. Vigil-Galán O, Courel M, Espindola-Rodriguez M, Izquierdo-Roca V, Saucedo E, Fairbrother A. Toward a high Cu_2ZnSnS_4 solar cell efficiency processed by spray pyrolysis method. Journal of Renewable and Sustainable Energy, 2013, 5(5): 053137
8. Yeh M Y, Lee C C, Wuu D S. Influences of synthesizing temperatures on the properties of Cu_2ZnSnS_4 prepared by sol–gel spin-coated deposition. Journal of Sol-Gel Science and Technology, 2009, 52(1): 65–68
9. Jiang M, Lan F, Yan X, Li G. $Cu_2ZnSn(S_{1-x}Se_x)_4$thin film solar cells prepared by water-based solution process. Physica Status Solidi (RRL)- Rapid Research Letters, 2014, 8(3): 223–227
10. Jiang M, Li Y, Dhakal R, Thapaliya P, Mastro M, Caldwell J, Kub F, Yan X. Cu_2ZnSnS_4 polycrystalline thin films with large densely packed grains prepared by sol-gel method. Journal of Photonics for Energy, 2011, 1(1): 019501
11. Tian Q, Huang L, Zhao W, Yang Y, Wang G, Pan D. Metal sulfide precursor aqueous solutions for fabrication of Cu2ZnSn(S,Se)$_4$ thin film solar cells. Green Chemistry, 2015, 17(2): 1269–1275
12. Kishore Kumar Y B, Suresh Babu G, Uday Bhaskar P, Sundara Raja V. Preparation and characterization of spray-deposited Cu_2ZnSnS_4 thin films. Solar Energy Materials and Solar Cells, 2009, 93(8): 1230–1237
13. Zhong J, Xia Z, Zhang C, Li B, Liu X, Cheng Y B, Tang J. One-pot synthesis of self-stabilized aqueous nanoinks for $Cu_2ZnSn(S,Se)_4$ solar cells. Chemistry of Materials, 2014, 26(11): 3573–3578
14. Woo K, Kim Y, Moon J. A non-toxic, solution-processed, earth abundant absorbing layer for thin-film solar cells. Energy & Environmental Science, 2012, 5(1): 5340–5345
15. Larramona G, Bourdais S, Jacob A, Choné C, Muto T, Cuccaro Y, Delatouche B, Moisan C, Péré D, Dennler G. Efficient Cu_2ZnSnS_4 solar cells spray coated from a hydro-alcoholic colloid synthesized by instantaneous reaction. RSC Advances, 2014, 4(28): 14655–14662
16. Larramona G, Bourdais S, Jacob A, Choné C, Muto T, Cuccaro Y, Delatouche B, Moisan C, Péré D, Dennler G. 8.6% efficient CZTSSe solar cells sprayed from water–ethanol CZTS colloidal solutions. Journal of Physical Chemistry Letters, 2014, 5(21): 3763–3767
17. Li Z, Ho J C W, Lee K K, Zeng X, Zhang T, Wong L H, Lam Y M. Environmentally friendly solution route to kesterite $Cu_2ZnSn(S,Se)_4$ thin films for solar cell applications. RSC Advances, 2014, 4(51): 26888–26894
18. Chen G, Yuan C, Liu J, Huang Z, Chen S, Liu W, Jiang G, Zhu C. Fabrication of Cu_2ZnSnS_4 thin films using oxides nanoparticles ink for solar cell. Journal of Power Sources, 2015, 276: 145–152
19. van Embden J, Chesman A S, Della Gaspera E, Duffy N W, Watkins S E, Jasieniak J J. $Cu_2ZnSnS_{4x}Se_{4(1-x)}$ solar cells from polar nanocrystal inks. Journal of the American Chemical Society, 2014, 136(14): 5237–5240
20. Kang C C, Chen H F, Yu T C, Lin T C. Aqueous synthesis of wurtzite Cu_2ZnSnS_4 nanocrystals. Materials Letters, 2013, 96: 24–26
21. Kush P, Ujjain S K, Mehra N C, Jha P, Sharma R K, Deka S. Development and properties of surfactant-free water-dispersible Cu_2ZnSnS_4 nanocrystals: a material for low-cost photovoltaics. Chemphyschem: a European journal of Chemical Physics and

Physical Chemistry, 2013, 14(12): 2793–2799
22. Liu W, Guo B, Mak C, Li A, Wu X, Zhang F. Facile synthesis of ultrafine Cu_2ZnSnS_4 nanocrystals by hydrothermal method for use in solar cells. Thin Solid Films, 2013, 535: 39–43
23. Tian Q, Xu X, Han L, Tang M, Zou R, Chen Z, Yu M, Yang J, Hu J. Hydrophilic Cu_2ZnSnS_4 nanocrystals for printing flexible, low-cost and environmentally friendly solar cells. CrystEngComm, 2012, 14 (11): 3847–3850
24. Hsu K C, Liao J D, Chao L M, Fu Y S. Fabrication and characterization of Cu_2ZnSnS_4 powders by a hydrothermal method. Japanese Journal of Applied Physics, 2013, 52(6R): 061202
25. Camara S M, Wang L, Zhang X. Easy hydrothermal preparation of Cu_2ZnSnS_4 (CZTS) nanoparticles for solar cell application. Nanotechnology, 2013, 24(49): 495401
26. Jiang H, Dai P, Feng Z, Fan W, Zhan J. Phase selective synthesis of metastable orthorhombic Cu_2ZnSnS_4. Journal of Materials Chemistry, 2012, 22(15): 7502–7506
27. Tiong V T, Bell J, Wang H. One-step synthesis of high quality kesterite Cu_2ZnSnS_4 nanocrystals- a hydrothermal approach. Beilstein Journal of Nanotechnology, 2014, 5: 438–446
28. Tiong V T, Zhang Y, Bell J, Wang H. Phase-selective hydrothermal synthesis of Cu_2ZnSnS_4 nanocrystals: the effect of the sulphur precursor. CrystEngComm, 2014, 16(20): 4306–4313
29. Zhao Y, Zhou W H, Jiao J, Zhou Z J, Wu S X. Aqueous synthesis and characterization of hydrophilic Cu_2ZnSnS_4 nanocrystals. Materials Letters, 2013, 96: 174–176
30. Kovalenko M V, Scheele M, Talapin D V. Colloidal nanocrystals with molecular metal chalcogenide surface ligands. Science, 2009, 324(5933): 1417–1420
31. Kovalenko M V, Bodnarchuk M I, Zaumseil J, Lee J S, Talapin D V. Expanding the chemical versatility of colloidal nanocrystals capped with molecular metal chalcogenide ligands. Journal of the American Chemical Society, 2010, 132(29): 10085–10092
32. Jiang C, Lee J S, Talapin D V. Soluble precursors for $CuInSe_2$, $CuIn_{1-x}Ga_xSe_2$, and $Cu_2ZnSn(S,Se)_4$ based on colloidal nanocrystals and molecular metal chalcogenide surface ligands. Journal of the American Chemical Society, 2012, 134(11): 5010–5013
33. Zhou H, Duan H S, Yang W, Chen Q, Hsu C J, Hsu W C, Chen C C, Yang Y. Facile single-component precursor for Cu_2ZnSnS_4 with enhanced phase and composition controllability. Energy & Environmental Science, 2014, 7(3): 998–1005
34. Su Z, Sun K, Han Z, Cui H, Liu F, Lai Y, Li J, Hao X, Liu Y, Green M A. Fabrication of Cu_2ZnSnS_4 solar cells with 5.1% efficiency via thermal decomposition and reaction using a non-toxic sol–gel route. Journal of Materials Chemistry. A, Materials for Energy and Sustainability, 2014, 2(2): 500–509
35. Kim S, Kim J. Effect of selenization on sprayed Cu_2ZnSnS_4 thin film solar cell. Thin Solid Films, 2013, 547: 178–180
36. Scragg J J, Berg D M, Dale P J A. 3.2% efficient Kesterite device from electrodeposited stacked elemental layers. Journal of Electroanalytical Chemistry, 2010, 646(1–2): 52–59
37. Araki H, Kubo Y, Mikaduki A, Jimbo K, Maw W S, Katagiri H, Yamazaki M, Oishi K, Takeuchi A. Preparation of Cu_2ZnSnS_4 thin films by sulfurizing electroplated precursors. Solar Energy Materials and Solar Cells, 2009, 93(6–7): 996–999
38. Scragg J J, Dale P J, Peter L M. Towards sustainable materials for solar energy conversion: preparation and photoelectrochemical characterization of Cu_2ZnSnS_4. Electrochemistry Communications, 2008, 10(4): 639–642
39. Scragg J J, Dale P J, Peter L M. Synthesis and characterization of Cu_2ZnSnS_4 absorber layers by an electrodeposition-annealin88g route. Thin Solid Films, 2009, 517(7): 2481–2484
40. Iljina J, Zhang R, Ganchev M, Raadik T, Volobujeva O, Altosaar M, Traksmaa R, Mellikov E. Formation of Cu_2ZnSnS_4 absorber layers for solar cells by electrodeposition-annealing route. Thin Solid Films, 2013, 537: 85–89
41. Ennaoui A, Lux-Steiner M, Weber A, Abou-Ras D, Kötschau I, Schock H W, Schurr R, Hölzing A, Jost S, Hock R, Voß T, Schulze J, Kirbs A. Cu_2ZnSnS_4 thin film solar cells from electroplated precursors: Novel low-cost perspective. Thin Solid Films, 2009, 517 (7): 2511–2514
42. Wang Y, Ma J, Liu P, Chen Y, Li R, Gu J, Lu J, Yang S, Gao X. Cu_2ZnSnS_4 films deposited by a co-electrodeposition-annealing route. Materials Letters, 2012, 77: 13–16
43. Pawar S M, Pawar B S, Moholkar A V, Choi D S, Yun J H, Moon J H, Kolekar S S, Kim J H. Single step electrosynthesis of Cu_2ZnSnS_4 (CZTS) thin films for solar cell application. Electrochimica Acta, 2010, 55(12): 4057–4061
44. Schurr R, Hölzing A, Jost S, Hock R, Voß T, Schulze J, Kirbs A, Ennaoui A, Lux-Steiner M, Weber A, Kötschau I, Schock H W. The crystallisation of Cu_2ZnSnS_4 thin film solar cell absorbers from co-electroplated Cu – Zn – Sn precursors. Thin Solid Films, 2009, 517 (7): 2465–2468
45. Chan C P, Lam H, Surya C. Preparation of Cu_2ZnSnS_4 films by electrodeposition using ionic liquids. Solar Energy Materials and Solar Cells, 2010, 94(2): 207–211
46. Mali S S, Patil B M, Betty C A, Bhosale P N, Oh Y W, Jadkar S R, Devan R S, Ma Y R, Patil P S. Novel synthesis of kesterite Cu_2ZnSnS_4 nanoflakes by successive ionic layer adsorption and reaction echnique: characterization and application. Electrochimica Acta, 2012, 66: 216–221
47. Mali S S, Shinde P S, Betty C A, Bhosale P N, Oh Y W, Patil P S. Synthesis and characterization of Cu_2ZnSnS_4 thin films by SILAR method. Journal of Physics and Chemistry of Solids, 2012, 73(6): 735–740
48. Shinde N M, Dubal D P, Dhawale D S, Lokhande C D, Kim J H, Moon J H. Room temperature novel chemical synthesis of Cu_2ZnSnS_4 (CZTS) absorbing layer for photovoltaic application. Materials Research Bulletin, 2012, 47(2): 302–307
49. Shinde N M, Deshmukh P R, Patil S V, Lokhande C D. Aqueous chemical growth of Cu_2ZnSnS_4 (CZTS) thin films: air annealing and photoelectrochemical properties. Materials Research Bulletin, 2013, 48(5): 1760–1766
50. Patel K, Shah D V, Kheraj V. Influence of deposition parameters and annealing on Cu_2ZnSnS_4 thin films grown by SILAR. Journal of Alloys and Compounds, 2015, 622: 942–947
51. Su Z, Yan C, Sun K, Han Z, Liu F, Liu J, Lai Y, Li J, Liu Y. Preparation of Cu_2ZnSnS_4 thin films by sulfurizing stacked precursor thin films via successive ionic layer adsorption and reaction method. Applied Surface Science, 2012, 258(19): 7678–7682
52. Gao C, Shen H, Jiang F, Guan H. Preparation of Cu_2ZnSnS_4 film by

sulfurizing solution deposited precursors. Applied Surface Science, 2012, 261: 189–192
53. Wangperawong A, King J S, Herron S M, Tran B P, Pangan-Okimoto K, Bent S F. Aqueous bath process for deposition of Cu_2ZnSnS_4 photovoltaic absorbers. Thin Solid Films, 2011, 519(8): 2488–2492
54. Moriya K, Tanaka K, Uchiki H. Characterization of Cu_2ZnSnS_4thin films prepared by photo-chemical deposition. Japanese Journal of Applied Physics, 2005, 44(1B): 715–717
55. Shinde N M, Lokhande C D, Kim J H, Moon J H. Low cost and large area novel chemical synthesis of Cu_2ZnSnS_4 (CZTS) thin films. Journal of Photochemistry and Photobiology A Chemistry, 2012, 235: 14–20
56. Chen S, Walsh A, Gong X G, Wei S H. Classification of lattice defects in the kesterite Cu2ZnSnS$_4$ and $Cu_2ZnSnSe_4$ earth-abundant solar cell absorbers. Advanced Materials, 2013, 25(11): 1522–1539
57. Hergert F, Hock R. Predicted formation reactions for the solid-state syntheses of the semiconductor materials Cu_2Sn*X*$_3$ and Cu_2ZnSn*X*$_4$ (*X* = S, Se) starting from binary chalcogenides. Thin Solid Films, 2007, 515(15): 5953–5956
58. Shin S W, Pawar S M, Park C Y, Yun J H, Moon J H, Kim J H, Lee J Y. Studies on Cu_2ZnSnS_4 (CZTS) absorber layer using different stacking orders in precursor thin films. Solar Energy Materials and Solar Cells, 2011, 95(12): 3202–3206
59. Mitzi D B, Gunawan O, Todorov T K, Wang K, Guha S. The path towards a high-performance solution-processed kesterite solar cell. Solar Energy Materials and Solar Cells, 2011, 95(6): 1421–1436
60. Polizzotti A, Repins I L, Noufi R, Wei S H, Mitzi D B. The state and future prospects of kesterite photovoltaics. Energy & Environmental Science, 2013, 6(11): 3171–3182
61. Vigil-Galán O, Courel M, Andrade-Arvizu J A, Sánchez Y, Espíndola-Rodríguez M, Saucedo E, Seuret-Jiménez D, Titsworth M. Route towards low cost-high efficiency second generation solar cells: current status and perspectives. Journal of Materials Science Materials in Electronics, 2015, 26(8): 5562–5573
62. Chen S, Gong X G, Walsh A, Wei S H. Defect physics of the kesterite thin-film solar cell absorber Cu_2ZnSnS_4. Applied Physics Letters, 2010, 96(2): 021902
63. Vigil-Galán O, Espíndola-Rodríguez M, Courel M, Fontané X, Sylla D, Izquierdo-Roca V, Fairbrother A, Saucedo E, Pérez-Rodríguez A. Secondary phases dependence on composition ratio in sprayed Cu_2ZnSnS_4 thin films and its impact on the high power conversion efficiency. Solar Energy Materials and Solar Cells, 2013, 117: 246–250
64. Wen Q, Li Y, Yan J, Wang C. Crystal size-controlled growth of Cu_2ZnSnS_4 films by optimizing the Na doping concentration. Materials Letters, 2015, 140: 16–19
65. Prabhakar T, Jampana N. Effect of sodium diffusion on the structural and electrical properties of Cu_2ZnSnS_4 thin films. Solar Energy Materials and Solar Cells, 2011, 95(3): 1001–1004
66. Tong Z, Yan C, Su Z, Zeng F, Yang J, Li Y, Jiang L, Lai Y, Liu F. Effects of potassium doping on solution processed kesterite Cu_2ZnSnS_4 thin film solar cells. Applied Physics Letters, 2014, 105(22): 223903
67. Johnson M, Baryshev S V, Thimsen E, Manno M, Zhang X, Veryovkin I V, Leighton C, Aydil E S. Alkali-metal-enhanced grain growth in Cu_2ZnSnS_4thin films. Energy & Environmental Science, 2014, 7(6): 1931–1938
68. Zhou H, Song T B, Hsu W C, Luo S, Ye S, Duan H S, Hsu C J, Yang W, Yang Y. Rational defect passivation of $Cu_2ZnSn(S,Se)_4$ photovoltaics with solution-processed Cu_2ZnSnS_4:Na nanocrystals. Journal of the American Chemical Society, 2013, 135(43): 15998–16001
69. Nagaoka A, Miyake H, Taniyama T, Kakimoto K, Nose Y, Scarpulla M A, Yoshino K. Effects of sodium on electrical properties in Cu_2ZnSnS_4 single crystal. Applied Physics Letters, 2014, 104(15): 152101
70. Todorov T, Mitzi D B. Direct liquid coating of chalcopyrite light-absorbing layers for photovoltaic devices. European Journal of Inorganic Chemistry, 2010, 2010(1): 17–28
71. Zhong J, Xia Z, Luo M, Zhao J, Chen J, Wang L, Liu X, Xue D J, Cheng Y B, Song H, Tang J. Sulfurization induced surface constitution and its correlation to the performance of solution-processed $Cu_2ZnSn(S,Se)_4$ solar cells. Scientific Reports, 2014, 4: 6288–6296
72. Walter T, Herberholz R, Müller C, Schock H W. Determination of defect distributions from admittance measurements and application to $Cu(In,Ga)Se_2$ based heterojunctions. Journal of Applied Physics, 1996, 80(8): 4411
73. Shin B, Bojarczuk N A, Guha S. On the kinetics of $MoSe_2$ interfacial layer formation in chalcogen-based thin film solar cells with a molybdenum back contact. Applied Physics Letters, 2013, 102(9): 091907
74. Cui H, Lee C Y, Li W, Liu X, Wen X, Hao X. Improving efficiency of evaporated Cu_2ZnSnS_4 thin film solar cells by a thin Ag intermediate layer between absorber and back contact. International Journal of Photoenergy, 2015, 170507
75. Liu X, Cui H, Li W, Song N, Liu F, Conibeer G, Hao X. Improving Cu_2ZnSnS_4 (CZTS) solar cell performance by an ultrathin ZnO intermediate layer between CZTS absorber and Mo back contact. Physica Status Solidi (RRL)- Rapid Research Letters, 2014, 8(12): 966–970
76. Shin B, Gunawan O, Zhu Y, Bojarczuk N A, Chey S J, Guha S. Thin film solar cell with 8.4% power conversion efficiency using an earth-abundant Cu_2ZnSnS_4 absorber. Progress in Photovoltaics: Research and Applications, 2013, 21(1): 72–76
77. Liu F, Sun K, Li W, Yan C, Cui H, Jiang L, Hao X, Green M A. Enhancing the Cu_2ZnSnS_4 solar cell efficiency by back contact modification: inserting a thin TiB_2 intermediate layer at Cu_2ZnSnS_4/Mo interface. Applied Physics Letters, 2014, 104(5): 051105

Cheng Zhang was an undergraduate student at Wuhan National Laboratory for Optoelectronics (WNLO) at Huazhong University of Science and Technology. He obtained his bachelor degree under the supervision of Dr. Jie Zhong and Prof. Jiang Tang from 2014 to 2015. He will start his Ph.D. study in Prof. Jian Lin's group at the Department of Mechanical & Aerospace Engineering at University of Missouri-Columbia. His research

focuses on advanced materials synthesis and processing.

Jie Zhong currently is an associate professor at State Key Laboratory of Advanced Technology for Materials Synthesis and Processing, Wuhan University of Technology (WHUT). Before that, he worked at Wuhan National Laboratory for Optoelectronics (WNLO) at Huazhong University of Science and Technology (HUST) as a postdoctoral researcher and lecturer. He received his Ph.D. degree in materials science and engineering in Central South University (CSU) in 2012. From 2008 to 2012, he conducted research as a visiting student and later as a research assistant at Department of Materials Engineering in Monash University. Jie's research interest is now focused on synthesizing green inks of semiconductors (copper zinc tin sulfoselenide, perovskite and etc.), and producing photovoltaic and sensing devices via printing routes.

Jiang Tang is now a professor at Wuhan National Laboratory for Optoelectronics, Huazhong University of Science and Technology. He received his bachelor's degree from University of Science and Technology of China and his Ph.D. degree from University of Toronto in the Department of Materials Science and Engineering under the supervision of Prof. Edward H. Sargent. His research interest is chalcogenide thin film solar cells and colloidal quantum dot optoelectronic devices. He is the research pioneer of antimony selenide (Sb_2Se_3) thin film photovoltaics.